Interaction of a Novel GDP Exchange Inhibitor with the Ras Protein

Ashit K. Ganguly, Yu-Sen Wang,* Birendra N. Pramanik, Ronald J. Doll, Mark E. Snow, Arthur G. Taveras, Stacy Remiszewski, David Cesarz, J. del Rosario, Bancha Vibulbhan, Joan E. Brown, Paul Kirschmeier, Eric C. Huang, Larry Heimark, Anthony Tsarbopoulos, and Viyyoor M. Girijavallabhan

Schering-Plough Research Institute, 2015 Galloping Hill Road, Kenilworth, New Jersey 07033

Robert M. Aust, Edward L. Brown, Dorothy M. DeLisle, Shella A. Fuhrman, Thomas F. Hendrickson, Charles R. Kissinger, Robert A. Love, Wess A. Sisson, J. Ernest Villafranca, and Steve E. Webber

Agouron Pharmaceuticals, San Diego, California 92121

Received March 12, 1998; Revised Manuscript Received July 13, 1998

ABSTRACT: Mutated, tumorigenic Ras is present in a variety of human tumors. Compounds that inhibit tumorigenic Ras function may be useful in the treatment of Ras-related tumors. The interaction of a novel GDP exchange inhibitor (SCH-54292) with the Ras−GDP protein was studied by NMR spectroscopy. The binding of the inhibitor to the Ras protein was enhanced at low Mg^{2+} concentrations, which enabled the preparation of a stable complex for NMR study. To understand the enhanced inhibitor binding and the increased GDP dissociation rates of the Ras protein, the conformational changes of the Ras protein at low Mg^{2+} concentrations was investigated using two-dimensional $^{1}H-^{15}N$ HSQC experiments. The Ras protein existed in two conformations in slow exchange on the NMR time scale under such conditions. The conformational changes mainly occurred in the GDP binding pocket, in the switch I and the switch II regions, and were reversible. The Ras protein resumed its regular conformation after an excess amount of Mg^{2+} was added. A model of the inhibitor in complex with the Ras−GDP protein was derived from intra- and intermolecular NOE distance constraints, and revealed that the inhibitor bound to the critical switch II region of the Ras protein.

The Ras proteins play an important role in cell mitogenesis by the Ras activation−deactivation cycle (*1*−*4*). To induce mitogenesis, the Ras protein must be converted to the active or "turned-on" state by exchanging its bound GDP for GTP, known as the Ras nucleotide exchange process. The GDP−GTP nucleotide exchange process is one of the key activation steps regulating Ras function, and is an attractive target for therapeutic intervention for treatment of Ras-related tumors. The discovery of potent, non-nucleotide inhibitors of the Ras nucleotide exchange process has been described recently (*5*, *6*), which included a preliminary NMR analysis of a novel inhibitor, SCH-54292. Here, we describe the interaction of SCH-54292 (Figure 1A) with the Ras−GDP protein as studied by NMR spectroscopy. The binding of the inhibitor to the Ras protein was enhanced at low Mg^{2+} concentrations, which enables the preparation of a stable complex sample for NMR measurements. Numerous efforts to cocrystallize the potent nucleotide exchange inhibitor SCH-54292 (IC_{50} = 0.7 μM) with the Ras protein were unsuccessful. The bound conformation and the binding site of SCH-54292 in complex with the Ras protein were eventually derived from NMR experimental analysis in combination with the crystal structure of the Ras protein (*7*), molecular modeling, and mass spectrometry (*8*). The information presented here may provide insight into the nucleotide exchange process as well as help in the design of anti-Ras drugs.

EXPERIMENTAL PROCEDURES

Protein Expression. The C-terminally truncated human H-Ras (1−166) was expressed in *Escherichia coli* from a synthetic Ras gene under the control of both *lpp* and *taq* promoters (*9*), while Ras−GDP (1−166) was purified from fermentor-grown, IPTG-induced cells (*10*). The activity of this protein in GDP binding assays and GTPase assays was comparable to published data (*10*−*12*). Uniformly ^{15}N-labeled H-Ras (1−166) protein was expressed in *E. coli* grown in minimal medium (M9) supplemented with 1 mg/mL $^{15}NH_4Cl$ and 50 mg/L [^{15}N]arginine. The Ras−GDP protein was purified from cell paste via sequential chromatography on Fast Flow DEAE Sephadex and Sephadex G-100 resins.

Preparation of the Inhibitor−Ras Complex. The activity of SCH-54292 (IC_{50} = 0.7 μM) was determined in a GDP exchange assay in which the extent of the exchange of [^{32}P]-GDP by unlabeled GDP was measured in the presence of an inhibitor (*18*). The Ras protein samples were loaded onto a Sephadex G-25 column (Pharmacia, Uppsala, Sweden) to exchange to an NMR buffer. The NMR buffer contained 20 mM Tris-d_{11} and 40 mM NaCl in D_2O at pH 6.5. The inhibitor−protein complex was prepared by dissolving 12 mg of the Ras protein in 8 mL of Tris-d_{11} buffer previously saturated with SCH-54292 (solubility = 0.3 mM) and containing 0.32 mM EDTA in D_2O with no $MgCl_2$ added. Under these conditions, the ratio of the compound to the Ras protein was 3.8. The mixture was incubated at room

* To whom correspodence should be addressed.

10.1021/bi9805691 CCC: $15.00
Published on Web 10/22/1998

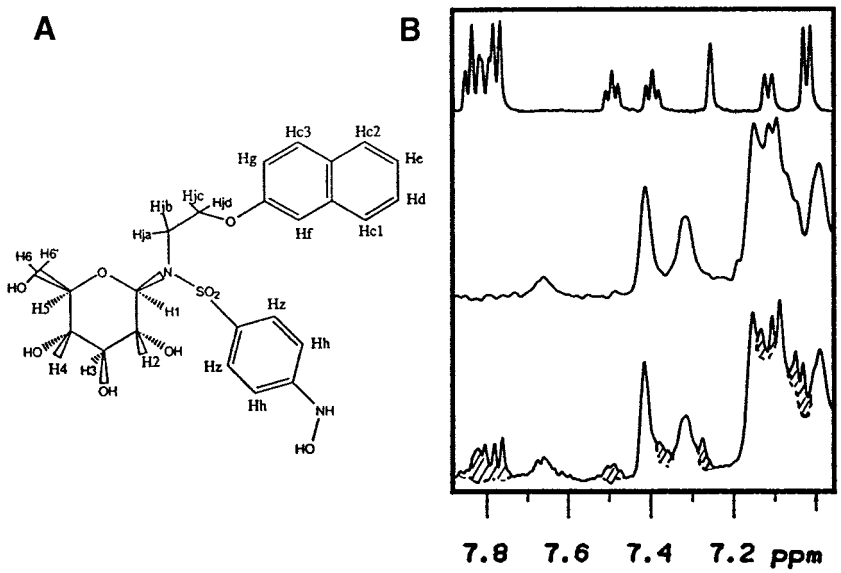

FIGURE 1: (A) Chemical structure and numbering of SCH-54292. (B) Expanded regions of proton spectra of SCH-54292 alone (top), the ^{15}N-labeled Ras−GDP protein (middle), and SCH-54292 in complex with the ^{15}N-labeled Ras−GDP protein (bottom). The cross-hatched areas represent signals of the bound SCH-54292 in the bottom spectrum. The latter two spectra were acquired with the (^{15}N)−H signals suppressed.

temperature for 20 min, and $MgCl_2$ was then added to a concentration of 5 mM. The sample was concentrated and further equilibrated with the buffer solution containing 20 mM Tris-d_{11}-DCl, 40 mM NaCl, and 5 mM $MgCl_2$ in D_2O (pH 6.5) using Centricon-10 microconcentrators (Amicon, Beverly, MA). The final Ras concentration was 1.3 mM when it was complexed with SCH-54292. For the two-dimensional ^{1}H−^{15}N HSQC experiments, the uniformly ^{15}N-labeled Ras protein was used following the same procedure as above.

NMR Spectroscopy. Proton NMR experiments carried out on the complex sample were performed at 500 MHz for ^{1}H on an Omega GN500 NMR spectrometer. DQF-COSY (*13*), TOSCY (*14*), and NOESY (*15*) spectra were recorded at 25.0 °C. An MLEV-17 spin lock sequence of 45 ms was employed in the TOCSY experiment. The NOESY spectrum was collected with a mixing time of 125 ms. NMR data were also collected for the Ras protein alone, as well as for the inhibitor under identical experimental conditions for comparison. The proton carrier was positioned on the water resonance, with spectral widths of 6515 Hz. Each set of experimental data was acquired with 2048 complex points and 512 FIDs, with 64 scans per FID. Quadrature detection was achieved via the method of States (*16*). The two-dimensional ^{1}H−^{15}N HSQC spectra for the uniformly ^{15}N-labeled Ras protein and its complex with SCH-54292 were acquired on a Varian Unity-plus 600 MHz NMR spectrometer. The transmitter was centered on the water signal for ^{1}H and at 117.25 ppm in the ^{15}N dimension. The proton spectra of the ^{15}N-labeled Ras and its complex with the inhibitor in Figure 1 were recorded using the isotope-filtered method (*17*). NMR data were exported to a Sun Sparc station and processed using the program Felix version 950 software (Molecular Simulations, Inc., San Diego, CA).

Structural Calculation. To determine the bound conformation, a Monte Carlo conformational search was performed (Macromodel 4.0, AMBER potentials) from 5000 starting conformations (iteration limit = 1000, 1.03 e^{-3} kJ mol^{-1} $Å^{-1}$ convergence criteria). The intramolecular NOE-derived distance was used with boundaries of ±0.6 Å. To define the binding site, the four intermolecular NOEs were used. To resolve the ambiguity in the assignments of the NOEs associated with the Ras proton signals, a geometric analysis of the intermolecular NOEs was performed using a program developed in-house. Energy minimization of the Ras−inhibitor complex was carried out using DISCOVER (Molecular Simulations, Inc.) with the cvff and AMBER force fields.

RESULTS AND DISCUSSION

Enhanced Inhibitor Binding of the Ras Protein at Low Mg^{2+} Concentrations. Sample preparation is critical to the success of the experiment. In an attempt to prepare the complex, an excess amount of SCH-54292 was added into a Ras−GDP protein sample and the mixture was shaken overnight at 5 °C. Comparison of the NMR spectrum of the mixture with that of the Ras protein alone revealed that the signals of SCH-54292 were weak and broad. In an improved procedure, a mixture of the Ras−GDP protein and SCH-54292 was incubated in the presence of EDTA. The removal of Mg^{2+} by EDTA partially unfolded the protein and induced an open conformation as suggeted by Hall and Self (*18*), thereby enhancing the binding of SCH-54292. Immediately after incubation, an excess amount of $MgCl_2$ was added to refold the Ras protein so that the inhibitor was "locked" in the protein. Using this procedure, the signal intensities of the bound SCH-54292 were enhanced (Figure 1B). Excess inhibitor was present at the incubation stage to ensure the complete complexation of the protein, and was removed after incubation by ultrafiltration. The formation of a stable complex of SCH-54292 with the Ras protein was evident from the line broadening of the signals of SCH-54292 in the presence of the Ras protein (Figure 1B). Comparison of the integrals of the Phe-28 Hϵ of the Ras protein with the resonance associated with SCH-54292 at 7.4 ppm suggested the formation of a 0.9:1 inhibitor−protein complex.

Conformational Changes of the Ras−GDP Protein at Low Mg^{2+} Concentrations. The dissociation of the bound GDP

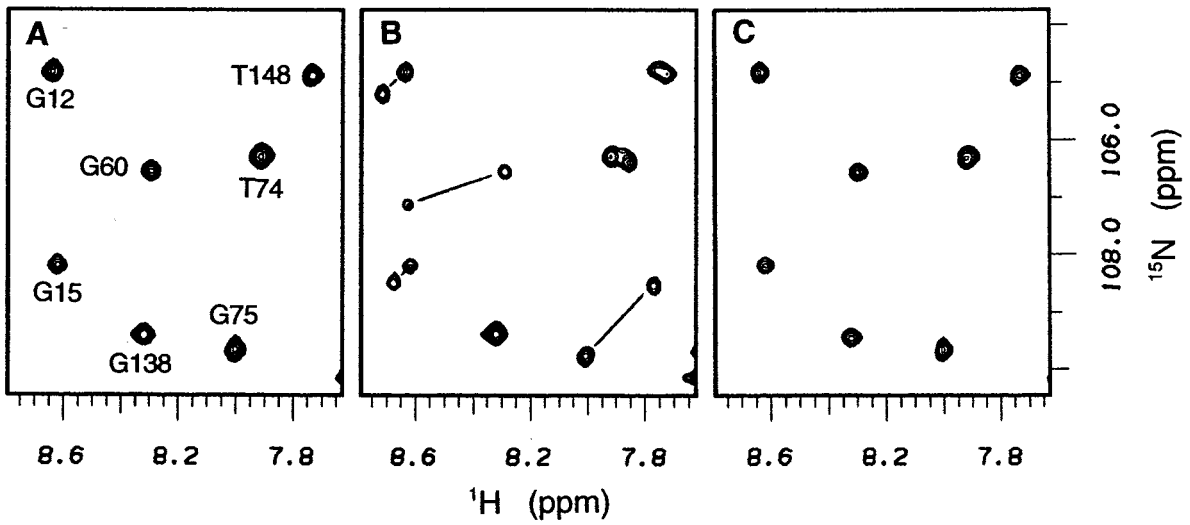

FIGURE 2: ^{1}H−^{15}N HSQC spectra of the Ras−GDP protein. (A) The sample was 1 mM ^{15}N-labeled Ras protein in 20 mM Tris-d_{11}-DCL buffer at pH 6.5. (B) EDTA was added to sample A to a concentration of 4 mM. (C) $MgCl_2$ was added to sample B to a concentration of 5 mM. In panel B, resonances from residues in the phosphate-binding loop (G12 and G15), in the switch II region (G60, T74, and G75), and near the base recognition regions (T148) were split, while G138 which does not belong to a binding site was unchanged. In panel C, after an excess amount of Mg^{2+} was added, the correlation peaks returned to the same position as in panel A.

was investigated by a numer of research groups (*18*−*21*). It was discovered that the dissociation rate of bound GDP of the Ras protein was greatly increased at low Mg^{2+} concentrations. However, no structural studies were conducted under such conditions. To understand the increased dissociation rate of GDP and the enhanced inhibitor binding reported here, the conformational changes of the Ras protein under such low-Mg^{2+} concentration conditions were monitored by ^{1}H−^{15}N HSQC experiments. The ^{1}H and ^{15}N chemical shift changes in a ^{1}H−^{15}N HSQC spectra provide evidence of structural changes. Figure 2 shows two-dimensional ^{1}H−^{15}N HSQC spectra of the Ras protein under various conditions. At low Mg^{2+} concentrations (Figure 2B), many ^{1}H−^{15}N correlation peaks were split into two peaks. While one set of peaks had the same chemical shifts of the folded active Ras protein as in Figure 2A, a new set of peaks had different chemical shifts, indicating the existence of a new conformation of the Ras protein. Thus, the Ras protein existed in two conformations in slow exchange on the NMR time scale at low Mg^{2+} concentrations. Careful examination revealed that these conformation changes were associated with residues in the GDP binding pocket, in the switch I and switch II regions. Upon addition of excess Mg^{2+}, these split peaks returned to their original positions (Figure 2C), suggesting that the conformational changes were reversible. These local conformational changes or an open conformation of the Ras protein (*18*) may facilitate the fast GDP exchange (*18*−*21*) and enhance the binding of the inhibitor. These results provided a structural basis for the understanding of the GDP exchange process as well as for the understanding of inhibitor binding. The effect of Mg^{2+} on the interaction of EF-Ts with EF-Tu by reducing the affinity of EF-Tu for guanine nucleotide was recently reported (*22*).

Conformation of the Inhibitor Bound to the Ras Protein. The proton resonances of the bound SCH-54292 were assigned from the two-dimensional DQF-COSY and two-dimensional TOCSY spectra. The principal source of structural information was derived from the two-dimensional NOESY data of the inhibitor−Ras complex. Careful comparison of the two-dimensional NOESY spectrum (Figure 3) of the complex with that of the Ras protein alone revealed a number of new NOE cross-peaks. A total of 29 interproton distances (Table 1) calculated from intramolecular NOEs was used to determine the conformation of SCH-54292. A Monte Carlo conformational analysis of these NOE-derived distances was performed, resulting in a bound conformation which satisfied the experimentally determined distance constraints (Figure 4).

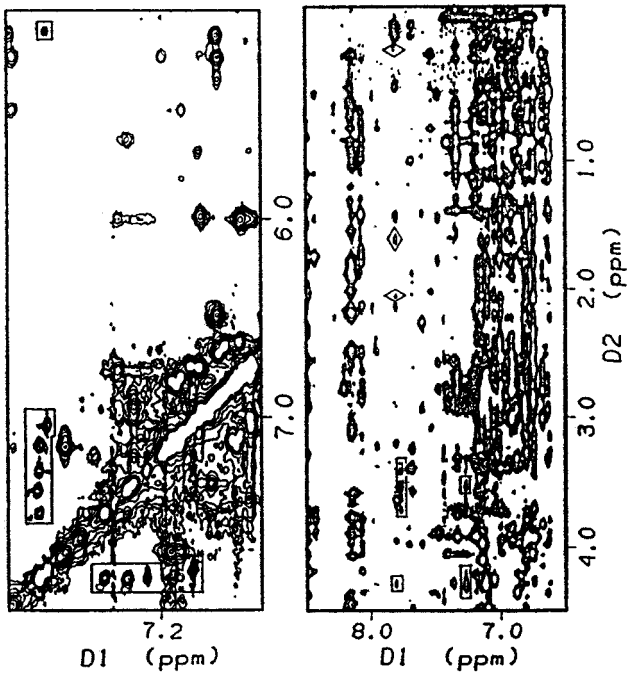

FIGURE 3: Two expanded regions of the two-dimensional NOESY spectrum of SCH-54292 complexed with the Ras−GDP protein collected with a 125 ms mixing time. The intramolecular NOE cross-peaks of the bound SCH-54292 are indicated by rectangular boxes. The intermolecular NOE cross-peaks between SCH-54292 and the Ras protein are represented by diamonds.

Chemical Shift Assignments of the Ras Protein Complexed with the Inhibitor. The backbone ^{1}H and ^{15}N chemical shifts

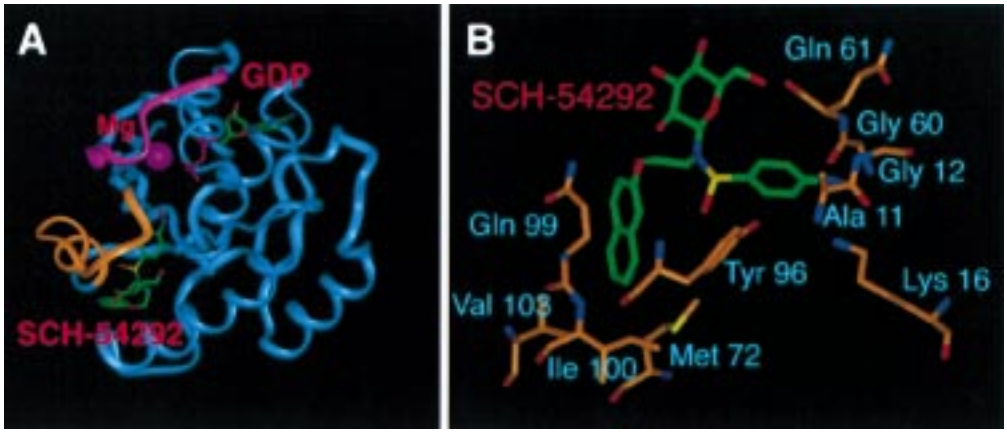

FIGURE 4: Interaction of SCH-54292 with the Ras−GDP protein. (A) The bound conformation of SCH-54292 and the overall structure of the ternary complex between the Ras protein (blue ribbon), GDP (green and purple), SCH-54292 (green), and the magnesium ion (purple). The switch I region is burgundy and the switch II region orange. (B) Closeup of the interaction of SCH-54292 (green) with the Ras protein (brown).

Table 1: Intramolecular Distance Restraints and Interproton Distances in the Model of SCH-54292 Bound to the Ras Protein

assignment	distance restraint	distance in model[a]
Hc1−Hd	2.5	2.5 (reference)
Hc1−Hf	2.5	2.5
Hc2−He	2.5	2.5
Hc3−Hg	2.5	2.5
Hz−Hh	2.5	2.5
Hz−Hf	VW[b]	5.8
Hz−H1	3.2	3.2
Hc1−Hjc	4.4	4.8
Hz−Hja	2.9	2.7
Hz−Hjb	3.4	3.3
Hz−H5	3.5	3.8
Hz−H6	3.9	4.2
Hf−Hja	3.9	4.1
Hf−Hjb	2.9	2.6
Hf−Hjc	2.4	2.5
Hf−H2	VW[b]	5.2
Hd−He	2.5	2.5
Hjd−Hjb	2.9	3.0
Hjd−H2	2.8	2.4
Hjd−H6′	4.4	4.9
Hja−Hjb	2.2	1.8
Hja−H6	3.9	4.3
H1−H2	3.4	3.1
H1−H3	2.6	2.5
H1−H5	2.4	2.4
H6−H4	2.2	2.7
H6−H6′	2.1	1.8
H3−H5	2.4	2.7
H6′−H5	2.3	2.6

[a] From the model of SCH-54292 in complex with the Ras protein. [b] VW denotes very weak.

of the Ras protein in complex with the inhibitor were measured in a two-dimensional $^1H-^{15}N$ HSQC spectrum. The assignments of the backbone resonances of the Ras protein in complex with the inhibitor are given in Table 2. Comparison of the chemical shifts of the complex with that of the Ras protein alone revealed that the differences in the ^1H and ^{15}N chemical shifts are small. The small differences in chemical shifts provided evidence that the backbone structure of the protein was not changed upon the binding of the inhibitor. This is consistent with the observed intermolecular NOEs which showed that the interaction occurred mainly between the small inhibitor and the side chains of the amino acid residues of the protein.

Binding Site Determination. In addition to intramolecular NOEs, four intermolecular NOEs between the inhibitor and the protein were unambiguously identified and assigned (represented by diamonds in Figure 3). The four NOEs resonated at 7.79−2.06, 7.79−1.61, 7.79−0.04, and 7.75−7.13 ppm (*D*1 and *D*2 ppm), respectively. The first three intermolecular NOEs were assigned to Hc1 or Hc3 of the naphthyl moiety of SCH-54292. The fourth NOE was assigned to Hz of the phenyl ring of the inhibitor. The published chemical shift assignments for the Ras−GDP protein (*23*, *24*) were used to assign the chemical shifts corresponding to the protons of the Ras proteins. The chemical shift differences between this work and the published work (*24*) were carefully examined by two-dimensional $^1H-^{15}N$ HSQC experiments of a uniformly ^{15}N-labeled Ras−GDP protein complexed with SCH-54292. The differences of the $(^{15}N)-^1H$ chemical shifts with respect to the published chemical shift values are less than 0.05 ppm.

A window of ±0.05 ppm was applied to the four chemical shifts (2.06, 1.61, 0.04, and 7.13 ppm) of the Ras protein to cover possible variation in chemical shifts due to differences in solution conditions and due to the formation of the complex with the inhibitor. A search of the published chemical shift assignments of the Ras protein (*23*, *24*) resulted in a number of possibilities at each chemical shift. To reduce the number of possibilities, the combinations of these NOEs were screened on the basis of simple geometry. While many amino acid residues of the Ras protein have associated protons which resonated at these chemical shifts, two protons of the Ras protein to simultaneously exhibit NOEs with two protons of SCH-54292 must satisfy a maximal distance limit between the attached carbons depending on the small size of the inhibitor. For example, for two Ras protons simultaneously exhibiting NOEs with Hc1 and Hc3, the distance between the attached Ras carbon atoms is defined by $D(ij) \leq \Sigma D_{Hc1-Hc3} + 2D_{C-H} + D_{NOE(i)} + D_{NOE(j)}$, where $D_{Hc1-Hc3}$ is the distance between Hc1 and Hc3 of SCH-54292 (5.52 Å), D_{C-H} is a Ras carbon−proton bond length (1.1 Å), and $D_{NOE(i)} + D_{NOE(j)}$ are the calculated distances from the interatomic NOEs observed between protons of the Ras protein and Hc1 and Hc3 of SCH-54292, respectively. For instance, the maximum distances between the two carbon atoms of the Ras protein for the first two NOEs must be

Table 2: Backbone Amide ^{1}H and ^{15}N Chemical Shifts of the Ras Protein (1−166) in Complex with the Inhibitor SCH-54292

residue	H^N	^{15}N	residue	H^N	^{15}N	residue	H^N	^{15}N
1 Met			57 Asp	8.48	127.68	113 Leu	8.86	127.36
2 Thr	8.97	123.51	58 Thr	6.78	108.67	114 Val	9.17	126.74
3 Glu	8.35	125.29	59 Ala	9.10	119.96	115 Gly	8.06	112.81
4 Tyr	8.73	120.31	60 Gly	8.28	106.53	116 Asn	8.73	119.69
5 Lys	9.14	122.98	61 Gln	8.58	117.56	117 Lys	7.34	110.58
6 Leu	9.45	124.71	62 Glu	8.76	119.15	118 Cys	8.77	112.74
7 Val	7.90	119.00	63 Glu	8.30	118.57	119 Asp	8.61	115.93
8 Val	8.93	127.44	64 Tyr	8.27	119.63	120 Leu	7.79	119.37
9 Val	9.16	119.11	65 Ser	7.84	118.25	121 Ala	8.13	121.25
10 Gly	7.13	106.04	66 Ala	8.74	110.73	122 Ala	7.66	120.17
11 Ala	9.14	122.98	67 Met	8.23	116.16	123 Arg	7.99	118.54
12 Gly	8.61	104.77	68 Arg	7.84	119.36	124 Thr	9.09	112.46
13 Gly	10.57	113.57	69 Asp	8.10	116.92	125 Val	7.62	122.99
14 Val	7.67	111.99	70 Gln	7.82	116.01	126 Glu	8.71	125.64
15 Gly	8.59	108.13	71 Tyr	8.24	118.35	127 Ser	9.40	120.20
16 Lys	10.59	123.98	72 Met	8.53	117.41	128 Arg	8.64	116.34
17 Ser	9.34	119.07	73 Arg	7.97	114.02	129 Gln	6.78	115.34
18 Ala	9.52	123.88	74 Thr	7.89	106.41	130 Ala	7.01	121.96
19 Leu	9.08	119.18	75 Gly	7.98	109.49	131 Gln	8.58	116.42
20 Thr	7.69	115.41	76 Glu	9.00	120.76	132 Asp	8.18	118.57
21 Ile	8.90	119.20	77 Gly	7.16	99.44	133 Leu	7.46	122.02
22 Gln	7.94	119.30	78 Phe	8.18	119.86	134 Ala	8.40	120.31
23 Leu	7.68	118.97	79 Leu	9.18	124.54	135 Arg	8.46	116.78
24 Ile	8.12	112.68	80 Cys	8.67	122.73	136 Ser	7.92	116.23
25 Gln	8.99	114.33	81 Val	8.97	124.50	137 Tyr	7.59	118.55
26 Asn	7.95	115.06	82 Phe	9.26	122.32	138 Gly	8.30	109.44
27 His	6.80	119.64	83 Ala	8.67	119.53	139 Ile	8.05	111.67
28 Phe	8.60	121.02	84 Ile	8.46	111.73	140 Pro		
29 Val	7.68	124.53	85 Asn	7.86	115.60	141 Tyr	8.18	118.57
30 Asp	7.79	120.84	86 Asn	7.93	117.76	142 Ile	8.48	128.60
31 Glu	7.69	117.59	87 Thr			143 Glu	7.80	123.14
32 Tyr	8.81	124.14	88 Lys	8.44	122.56	144 Thr	8.74	110.73
33 Asp	7.86	127.32	89 Ser	8.06	112.81	145 Ser	8.83	111.12
34 Pro			90 Phe	7.39	123.12	146 Ala	9.12	130.91
35 Thr	8.98	108.53	91 Glu	8.47	120.16	147 Lys	7.00	114.57
36 Ile	6.85	119.42	92 Asp	8.45	115.76	148 Thr	7.70	104.84
37 Glu	8.41	130.38	93 Ile	7.57	119.10	149 Arg	7.82	116.95
38 Asp	8.16	122.92	94 His	7.83	115.21	150 Gln	7.82	122.72
39 Ser	8.39	112.47	95 Gln	7.43	115.31	151 Gly	8.91	113.71
40 Tyr	9.10	119.96	96 Tyr	7.52	117.66	152 Val	7.07	119.03
41 Arg	8.39	118.71	97 Arg	8.35	117.18	153 Glu	8.23	115.14
42 Lys	8.67	120.43	98 Glu	7.95	115.91	154 Asp	8.11	114.93
43 Gln	8.80	127.43	99 Gln	7.84	118.25	155 Ala	8.57	122.57
44 Val	9.09	119.34	100 Ile	7.77	118.42	156 Phe	7.19	110.89
45 Val	8.07	119.54	101 Lys	7.78	116.14	157 Tyr	9.60	117.71
46 Ile	8.13	124.21	102 Arg	7.78	116.14	158 Thr	8.51	115.55
47 Asp	9.53	129.09	103 Val	8.03	116.38	159 Leu	7.17	119.98
48 Gly	8.29	101.47	104 Lys	8.06	116.63	160 Val	7.51	117.33
49 Glu	7.69	120.90	105 Asp	7.99	119.10	161 Arg	8.13	117.67
50 Thr	8.89	124.51	106 Ser	7.47	107.52	162 Glu	8.13	116.69
51 Cys	9.45	122.53	107 Asp	8.35	120.54	163 Ile	8.10	120.42
52 Leu	8.73	120.52	108 Asp	8.41	119.64	164 Arg	8.34	117.01
53 Leu	9.00	122.05	109 Val	7.59	120.81	165 Gln	7.62	114.15
54 Asp	8.74	124.01	110 Pro			166 His	7.69	123.30
55 Ile	9.21	122.27	111 Met	8.13	121.25	lig GDP H1′	6.07	
56 Leu	8.77	126.20	112 Val	8.04	112.81			

less than 18.1 Å. This geometric considerations placed upper limits on the allowed distances between these two protons of the Ras protein. All the possible assignments for the protons of the Ras protein were examined against the bound conformation of SCH-54292, docked to the three-dimensional structure of the protein, which was solved to 2.1 Å resolution (*7*). The structures of the Ras−GDP proteins have previously been solved at high resolution by X-ray crystallography (*25*, *26*) and by NMR spectroscopy (*24*). It was demonstrated that the NMR structures of the protein are very similar to the crystal structures (*24*). Energy minimization of the complex resulted in a model which satisfied the NOE constraints and geometrical criteria. The first intermolecular NOE was assigned to Met-72 Hϵ and Gln-99 Hβ of the Ras protein. The second and third NOEs were assigned to Ile-100 Hγ12 and Ile-100 Hγ11 of the Ras protein, respectively. The fourth NOE was assigned to Tyr-96 Hδ.

Interaction of SCH-54292 with the Ras Protein. The resulting model of SCH-54292 in complex with the Ras−GDP protein is shown in Figure 4. The interatomic distances in the model were also included in Table 1. The binding site of SCH-54292 is in the vicinity of the critical switch II region. The switch I and the switch II regions are the two regions that change conformations when the Ras protein is converted from the inactive GDP bound state to the active GTP bound state (*25*). The structural differences between

Ras−GDP and Ras−GTP in aqueous solution were previously investigated by NMR (*27*−*30*). The conformational differences were found mainly in switch I (loop L2 and part of the β2-strand) and switch II region containing loop L4 and part of the helix α2 by X-ray crystallography (*25*, *31*, *32*). A closeup of the interaction is shown in Figure 4B. This structure places the naphthyl of SCH-54292 in a hydrophobic pocket formed by Met-72, Gln-99, Ile-100, and Val-103 of the protein. The phenyl is in the vicinity of Gln-61, Gly-60, Tyr-96, and Lys-16. The glucose is exposed on the exterior of the complex. The hydroxylamine extends into the pocket near the Mg^{2+} and the phosphate, in a region that is occupied by ordered waters in the crystal structure. The model suggests the possibility that the hydroxylamine could ligand the Mg^{2+}, thereby enhancing its binding affinity. The binding region was independently verified by studies involving electrospray ionization (ESI) mass spectroscopic studies (*6*). The observation that the nucleotide inhibitor binds to the switch II region is consistent with the mutation study of the Ras protein (*33*). It was found that the switch II region was directly involved in the interaction with guanine nucleotide exchange factor.

These results may provide a structural basis for understanding the mechanism of nucleotide exchange inhibition. It was proposed that the binding of the monoclonal antibody Y13-259 would freeze the conformation of the switch II region and thus prevent the GDP−GTP exchange (*25*). Perhaps SCH-54292 plays a similar role like the antibody in freezing the conformation of the switch II region and thereby inhibiting the nucleotide exchange process. On the basis of the information obtained for SCH-54292, a number of small organic molecules were synthesized with variations of functional groups to enhance the solubility of these compounds. Some of these compounds, for example, SCH-54341 and SCH-56407, were found to be active in in vitro assays, and also found to form a ternary complex with Ras−GDP (Ras−GDP:SCH-54341) as detected by ESI mass spectrmetry (*6*).

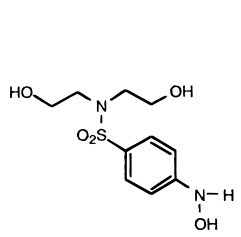

SCH-54341 (IC_{50} = 50 μM)

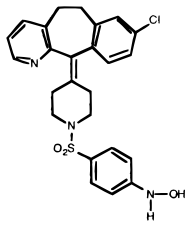

SCH-56407 (IC_{50} = 0.9 μM)

Figure 4 shows the naphthyl group of SCH-54292 interacts with a pocket formed by Met-72, Gln-99, and Ile-100 residues of the Ras protein. This lipophilic interaction seems to be important since SCH-54341, lacking this naphthyl group, has an IC_{50} of 50 μM compared to an IC_{50} of 0.7 μM for SCH 54292. However, SCH-56407 contains the lipophilic tricyclic heterocycle and retains a potency similar to that of SCH-54292 (IC_{50} of 0.9 μM vs an IC_{50} of 0.7 μM for SCH-54292).

We have presented the interaction of a non-nucleotide, small organic inhibitor that binds noncovalently to the Ras−GDP protein. The inhibitor binds to the Ras protein in a previously unidentified binding pocket without displacing the bound nucleotide. The structural information presented here should be useful for future anti-Ras drug design.

ACKNOWLEDGMENT

We thank Drs. T. M. Chan, C. A. Evans, M. M. Senior, and N. H. Yao for help and discussions during the course of the work and Soheil Rahmati for fermentation of the Ras protein.

REFERENCES

1. Barbacid, M. (1990) *Eur. J. Clin. Invest. 20*, 225−235.
2. Bourne, H. R., Sanders, D. A., and McCormick, F. (1990) *Nature 348*, 125−132.
3. Boguski, M., and McCormick, F. (1993) *Nature 366*, 643−654.
4. Quilliam, L. A., Khosravi-Far, R., Huff, S. Y., and Der, C. J. (1995) *BioEssays 17*, 395−404.
5. Taveras, A. G., Remiszewski, S., Doll, R. J., Cesarz, D., del Rosario, J., Vibulbhan, B., Bauer, B., Brown, J. E., Carr, D., Catino, J., Evans, C. A., Girijavallabhan, V., Huang, E. C., Heimark, L., James, L., Kirschmeier, P., Liberles, S., Nash, C., Perkins, L., Pramanik, B. N., Senior, M. M., Snow, M. E., Tsarbopoulos, A., Wang, Y.-S., Ganguly, A. K., Aust, R., Brown, E., Delisle, D., Fuhrman, S., Hendrickson, T., Kissinger, C., Love, R., Sisson, W. A., and Villafranca, E. (1997) *Bioorg. Med. Chem. 5*, 125−133.
6. Ganguly, A. K., Pramanik, B. N., Huang, E. C., Liberles, S., Heimark, L., Liu, Y. H., Tsarbopoulos, A., Doll, R. J., Taveras, A. G., Remiszewski, S., Snow, M. E., Wang, Y.-S., Vibulbhan, B., Cesarz, D., Brown, J. E., del Rosario, J., James, L., Kirschmeier, P., and Girijavallabhan, V. (1997) *Bioorg. Med. Chem. 5*, 817−820.
7. Love, R. (1998) Agouron Pharmaceuticals, personal communication. The X-ray crystallographic structure of the Ras−GDP protein used in this study was solved at 2.1 Å resolution, and in a novel space group such that the switch II loop does not have lattice contacts which could influence its conformation.
8. Ganguly, A. K., Pramanik, B. N., Tsarbopoulos, A., Covey, T. R., Huang, E. C., and Fuhrman, S. A. (1992) *J. Am. Chem. Soc. 114*, 6559−6560.
9. Ghrayeb, J., Kimura, H., Takahara, M., Hsiung, H., Masui, Y., and Inouye, M. (1984) *EMBO J. 3*, 2437−2442.
10. John, J., Schlichting, I., Schiltz, E., Rosch, P., and Wittinghofer, A. (1989) *J. Biol. Chem. 264*, 13086−13092.
11. Neal, S. E., Eccleston, J. F., Hall, A., and Webb, M. R. (1988) *J. Biol. Chem. 263*, 19718−19722.
12. Tucker, J., Sczakiel, G., Feuerstein, J., John, J., Goody, R. S., and Wittinghofer, A. (1986) *EMBO J. 5*, 1351−1358.
13. Rance, M., Sorenson, O. W., Bodenhausen, G., Wagner, G., Ernst, R. R., and Wuthrich, K. (1983) *Biochem. Biophys. Res. Commun. 117*, 479−485.
14. Davis, D. G., and Bax, A. (1985) *J. Am. Chem. Soc. 107*, 2820−2821.
15. Jeener, J., Meier, B. H., Bachmann, P., and Ernst, R. R. (1979) *J. Chem. Phys. 71*, 4546−4553.
16. States, D. J., Haberkorn, R. A., and Ruben, D. J. (1982) *J. Magn. Reson.*, 286−292.
17. Ikura, M., and Bax, A. (1992) *J. Am. Chem. Soc. 114*, 2433−2440.
18. Hall, A., and Self, A. J. (1986) *J. Biol. Chem. 261*, 10963−10965.
19. John, J., French, M., and Wittinghofer, A. (1988) *J. Biol. Chem. 263*, 11792−11799.
20. John, J., Rensland, H., Schlichting, I., Vetter, I., Borasio, G. D., Goody, R. S., and Wittinghofer, A. (1993) *J. Biol. Chem. 268*, 923−929.
21. Feuerstein, J., Kalbitzer, H. R., John, J., Goody, R. S., and Wittinghofer, A. (1997) *Eur. J. Biochem. 162*, 49−55.

22. Kawashima, T., Berthet-Colominas, C., Wulf, M., Cusack, S., and Leberman, R. (1996) *Nature 379*, 511−518.
23. Campbell-Burk, S. L., Domaille, P. J., Starovasnik, M. A., Boucher, W., and Laue, E. D. (1992) *J. Biomol. NMR 2*, 639−646.
24. Kraulis, P. J., Domaille, P. J., Campbell-Burk, S. L., Aken, T. V., and Laue, E. D. (1994) *Biochemistry 33*, 3515−3531.
25. Milburn, M. V., Tong, L., de Vos, A. M., Brunger, A., Yamaizumi, Z., Nishimura, S., and Kim, S.-H. (1990) *Science 247*, 939−945.
26. Tong, L., de Vos, A. M., Milburn, M. V., and Kim, S.-H. (1991) *J. Mol. Biol. 217*, 503−516.
27. Campbell-Burk, S. (1989) *Biochemistry 28*, 9478−9484.
28. Campbell-Burk, S., Papastavros, M. Z., McCormick, F., and Redfield, A. G. (1989) *Proc. Natl. Acad. Sci. U.S.A. 86*, 817−820.
29. Schlichting, I., John, J., Frech, M., Chardin, P., Wittinghofer, A., Zimmmerman, H., and Rosch, P. (1990) *Biochemistry 29*, 504−511.
30. Miller, A. F., Halkides, C. J., and Redfield, A. G. (1993) *Biochemistry 32*, 7367−7376.
31. Pai, E. F., Kabsch, W., Krengel, U., Holmes, K. C., John, J., and Wittinghofer, A. (1989) *Nature 341*, 209−214.
32. Schlichting, I., Almo, S. C., Rapp, G., Wilson, K., Petratos, K., Lentfer, A., Wittinghofer, A., Kabsch, W., Pai, E. F., Petsko, G. A., and Goody, R. S. (1990) *Nature 345*, 309−315.
33. Quilliam, L. A., Hisaka, M. M., Zhong, S., Lowry, A., Mosteller, R. D., Han, J., Drugan, J. K., Broek, D., Campbell, S. L., and Der, C. J. (1996) *J. Biol. Chem. 271*, 11076−11082.

BI9805691